Journal of Membrane Science 421–422 (2012) 180–189

Contents lists available at SciVerse ScienceDirect

Journal of Membrane Science

journal homepage: www.elsevier.com/locate/memsci

Characterisation of reverse osmosis permeates from municipal recycled water systems using fluorescence spectroscopy: Implications for integrity monitoring

Sachin Singh [a], Rita K. Henderson [a], Andy Baker [b], Richard M. Stuetz [a], Stuart J. Khan [a,*]

[a] UNSW Water Research Centre, School of Civil and Environmental Engineering, University of New South Wales, NSW 2052, Australia
[b] Connected Waters Initiative Research Centre, Water Research Laboratory, University of New South Wales, NSW 2052, Australia

ARTICLE INFO

Article history:
Received 30 October 2011
Received in revised form
19 May 2012
Accepted 12 July 2012
Available online 24 July 2012

Keywords:
Fluorescence
Reverse osmosis
Water recycling
Online monitoring
Probabilistic analysis

ABSTRACT

Reverse osmosis (RO) permeates from three Australian water recycling plants were characterised using three-dimensional excitation–emission matrix (EEM) fluorescence spectroscopy. The plants differed in terms of their RO operational configurations: RO feed water and pretreatment processes. Intermediate permeates from multiple staged RO treatment processes could be distinguished using Peak C ($\lambda_{Ex/Em}$= 340/426 nm) and Peak T_1 ($\lambda_{Ex/Em}$= 285/350 nm) fluorescence. Monte-Carlo analysis of Peak C and Peak T_1 rejection showed typical rejection of over 98% and permeate fluorescence intensities were used to determine Peak C as the most suitable for RO monitoring purposes. The results of this work indicate that fluorescence monitoring is a promising technique for sensitive quantitative and qualitative performance monitoring of RO treatment processes.

1. Introduction

High pressure filtration using reverse osmosis (RO) membranes is a proven and increasingly widely adopted technique for reclaiming very high quality water from wastewater sources [1]. Removal of many microbial and chemical contaminants is very effective under optimal operating conditions. The Australian guidelines for water recycling attribute greater than 6 log reduction of pathogens such as viruses to RO processes [2]. However, depending on specific solute, solution and membrane characteristics, as well as operational parameters such as temperature and flux, removal of some chemical and biological species can be variable [3]. This can be further exacerbated by performance issues such as membrane fouling and integrity loss [4,5]. The variable treatment performance for trace chemical and biological contaminants highlight the importance of monitoring the ongoing performance of RO treatment processes for some applications.

The most established online monitoring techniques for high pressure membrane treatment performance involve monitoring of electrical conductivity or total organic carbon (TOC) [6,7]. Electrical conductivity is a reliable and relatively inexpensive technique for monitoring the removal of ionic species. However, uncharged trace organic chemicals are not detected by conductivity measurement. Furthermore, it is known that such chemicals are typically rejected by different physical mechanisms to ionic species and thus conductivity is likely to be a poor surrogate measure for their removal [3].

TOC is a widely used bulk measurement of organic chemical species. A range of online TOC analysers are available on the market boasting low level organic carbon detection down to 20 ppb [8,9]. However, initial investment requirements for online TOC analysers are high and these do require regular maintenance making it costly for many utilities to implement [7].

TOC measurement does not distinguish between various fractions of the organic carbon and is thus not sufficiently sensitive to demonstrate significant log-removal of trace constituents. Accordingly, online TOC measurement is unlikely to be sufficiently sensitive for the detection of micro-changes in specific organic rejection within RO permeate concentrations. Furthermore, TOC measurement provides little insight into the character of the organic matter, which may further limit its usefulness for RO treatment performance monitoring [10].

Throughout the last decade, there has been rapidly growing interest in the development of fluorescence monitoring techniques for a wide range of water quality applications. Published investigations have covered a diverse range of applications, including river water quality monitoring [11], industrial wastewater monitoring [12] and the measurement of oil in water [13]. A recent literature review identified the strong potential of fluorescence monitoring for sensitive online assessment of recycled water quality and treatment process performance [14].

* Corresponding author. Tel.: +61 2 93855070.
E-mail address: s.khan@unsw.edu.au (S.J. Khan).

0376-7388/$ - see front matter © 2012 Elsevier B.V. All rights reserved.
http://dx.doi.org/10.1016/j.memsci.2012.07.008

In water analysis, fluorescence spectroscopy has recently been used as a tool for the characterisation of organic matter. Other characterisation tools such as organic carbon detection, ultraviolet spectroscopy (UV) and Fourier transform infrared spectroscopy (FTIR) have also been successfully used for this purpose [15–17]. Fluorescence is a rapid analytical technique that requires no reagents or sample preparation, and has previously been shown to achieve sensitivities 10–1000 times greater than those achieved by UV absorbance [18]. Spectroscopic data can be acquired within a few minutes as a three-dimensional matrix of excitation and emission wavelengths and emission intensity known as an excitation–emission matrix (EEM) [19].

Water quality analysis using fluorescence relies upon the presence of naturally fluorescing dissolved organic matter (fDOM). This is present in all natural sources of water and wastewater and has characteristic fluorescent signatures. The most commonly monitored fDOM are generally referred to as humic-like (Peak A: $\lambda_{Ex/Em}$= 237–260/400–500 nm; Peak C_1: $\lambda_{Ex/Em}$= 320–340/410–430 nm and Peak C_2: $\lambda_{Ex/Em}$=370–390/460–480 nm), tyrosine-like (Peak B_1:$\lambda_{Ex/Em}$= 225–237/309–321 nm and Peak B_2:$\lambda_{Ex/Em}$=275/310 nm), and tryptophan-like (Peak T_1: $\lambda_{Ex/Em}$= 275–290/340–360 nm and Peak T_2: $\lambda_{Ex/Em}$= 225–237/340–381 nm) [20,21]. These key fluorescence signals have previously been used to distinguish treated sewage effluent and river water [20], identify paper mill effluent in river water [22], and as a surrogate measure for biochemical oxygen demand (BOD) in municipal wastewaters [23].

Membrane systems have received some scrutiny using fluorescence spectroscopy. Several publications have focused on fouling in membrane bioreactors (MBR) for wastewater treatment [15,24–27]. Fluorescence spectroscopy has also been used to monitor and model the performance of membrane bioreactors [28,29]. Microfiltration (MF) and ultrafiltration (UF) membranes have been assessed using 3D fluorescence in order to understand fouling behaviour and characteristics of foulants [30,31]. The potential for organic chemical fouling of nanofiltration membranes during drinking water treatment was recently assessed using fluorescence spectroscopy to monitor membrane feed and permeate solutions. The authors of this study found fluorescence to be a highly sensitive technique, revealing more subtle variations in water quality than could be perceived by high performance size exclusion chromatography (HPSEC) [32]. Very little research has been reported on applications of fluorescence spectroscopy for monitoring RO membrane performance. However, preliminary investigations have suggested that the technique may be sufficiently sensitive to detect small variations in RO permeate qualities [33].

This paper presents fDOM signatures in RO permeate sourced from three different RO-based municipal water recycling plants in Australia. The objective was to establish a profile for future performance monitoring applications, and in doing so, identify fluorescence characteristics in RO permeates and the changes to these during the RO process. This in turn demonstrates the effectiveness of fluorescence in detecting subtle variations in RO treatment process performances. Parallel factor analysis (PARAFAC) of these data was published as part of a wider analysis [34]. Findings from that study established that multivariate data analysis methods such as PARAFAC, which are based on full fluorescence EEM characteristics, were not significantly more effective than the judicious use of single coordinate pairs in characterising wastewater and recycled water samples from a variety of sources.

The aim of this study is to identify optimum fluorescence peak(s) for online membrane integrity and underperformance monitoring. To do this, we have assessed fluorescence intensities from select excitation–emission coordinate pairs within the 3D fluorescence spectra. The results illustrate the potential for future online membrane performance monitoring applications using fluorescence spectroscopy.

2. Materials and methods

2.1. Water recycling plants

Three RO-based water recycling plants were monitored in this study. Two of these (Beenyup and St Marys) were pilot-scale plants constructed in order to optimise process performance for future full-scale water recycling plants. These plants receive final effluents from existing full-scale municipal wastewater treatment plants and treat the water for future high grade recycled water applications. The third plant (WRAMS) is a full-scale plant that treats a combination of stormwater and secondary effluent. A schematic illustration of the three water recycling plants showing approximate hourly flow rates and sampling locations is provided in Fig. 1.

2.1.1. WRAMS treatment plant

The water reclamation and management scheme (WRAMS) water treatment plant was constructed as part of a sustainable water management plan at Sydney Olympic Park for the 2000 Olympic Games. This plant features continuous-flow microfiltration (MF) and reverse osmosis (RO) membrane filters (filmtec BW30-FR) to treat a combination of stormwater and secondary

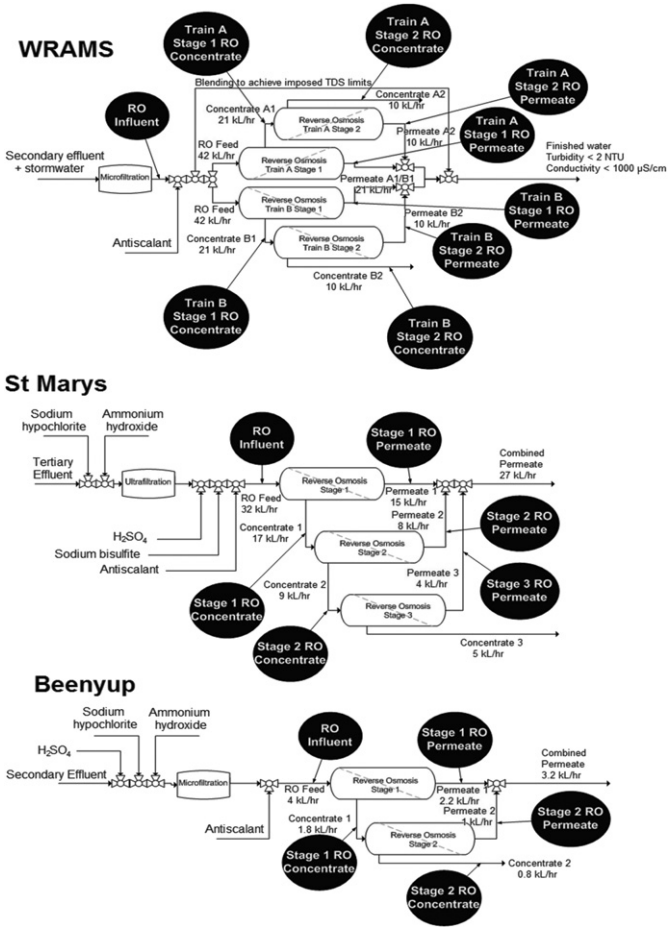

Fig. 1. Schematic diagrams of treatment process for the three advanced water recycling plants with sampling points illustrated.

Table 1
Fluorescence instrument parameters for Varian Cary Eclipse.

Method	Slit widths (nm)		PMT voltage (V)	Raman intensity of blank ($\lambda_{ex/em}$=348/393 nm)	No. of transient averages	Time for EEM completion (min)
	Ex	Em				
Low sensitivity	5	5	770–840	20 ± 2	1	1
High sensitivity	10	10	860–900	270 ± 8	3	5

effluent with a total capacity of 7.5 megalitres per day. All the water is filtered through the MF units while a maximum of 2 ML per day is further treated by RO. The finished water is a combination of both RO permeate and microfiltered water, blended in a non-specific ratio to maintain the final recycled water quality requirements. Chlorine is added as a disinfectant at the blending stage. This facility has two RO trains, each consisting of six Stage 1 modules and three Stage 2 modules. Generally, these trains are operated one at a time with the change-over occurring every 10 h.

2.1.2. St Marys pilot plant

St Marys advanced water treatment pilot plant was located on site at the St Marys sewage treatment plant at St Marys in Western Sydney, NSW. This pilot plant treated tertiary effluent from the St Marys STP, which was chloraminated prior to ultrafiltration (UF) followed by a 3-stage RO unit (Hydranautics ESPA2). The RO process was operated with a recovery of approximately 47% at each stage to give an overall combined recovery of around 84%.

2.1.3. Beenyup pilot RO plant

The Beenyup pilot RO plant was located on site at the Beenyup wastewater treatment plant in Perth, Western Australia. The pilot plant treated approximately 96 kl/day of secondary treated wastewater. The raw water was chloraminated by dosing 5:1 v/v ratio of sodium hypochlorite (12.5% solution) and ammonia (25% solution), the inlets for which are approximately 100 mm apart, directly into the raw water and allowing the formation of monochloramines in the raw water tank at a residence time of 3 h. This water was then treated by microfiltration (MF) followed by a 2-stage RO process (Hydranautics ESPA2) operated to achieve a combined recovery of 79–80%.

2.2. Sample collection

Triplicate grab samples were collected in fluorescent leachate-free 50 mL polypropylene containers. Samples from Beenyup pilot RO plant were collected on a weekly basis for 12 weeks during March–June, 2009. This sampling was conducted by onsite plant personnel and the samples were packed chilled in an ice box and shipped to the laboratory in Sydney by overnight courier. Samples from St Marys pilot RO plant were collected on eight nonconsecutive days within a 4 weeks period between November–December, 2008. Collection was undertaken by UNSW personnel and all samples were transported to the laboratory on the same day. Samples from WRAMS were also collected by UNSW personnel on a weekly basis for 12 weeks during April–June, 2010. This comprised of 4 weeks of samples from RO Train A and 8 weeks from RO Train B.

2.3. Sample analysis

Fluorescence EEMs were acquired on a Varian Cary Eclipse fluorescence spectrophotometer (Varian, Australia) using 1 cm pathlength (Starna) quartz cuvette at a scan speed of 9600 nm min^{-1}. Each EEM consisted of excitation wavelengths from 200 to 400 nm in stepwise increments of 5 nm and emission wavelengths from 280 to500 nm, in 2 nm increments. A low sensitivity method was used for samples obtained pre-RO whilst a high sensitivity method was used for post-RO samples. Specific instrument parameters used for these methods are detailed in Table 1.

Additional measurements of pH, electrical conductivity, UV absorbance and total organic carbon (TOC) were also acquired for all samples. Electrical conductivity and pH levels were measured with a HACH HQ14d portable meter (Biolab, Australia), and TOC was measured with a TOC-5000A analyser (Shimadzu, Australia). UV absorbance was measured on a Varian Cary 50 Win UV spectrophotometer (Varian, Australia).

2.4. Data analysis

2.4.1. EEM interpretation

All EEMs were post-processed using Matlab 2007b software (Mathworks, US). The first step in the process was a blank subtraction using a sealed cell containing purified water as supplied by Varian, Inc. This was followed by application of instrument specific excitation and emission correction factors and removal of Rayleigh–Tyndall and Raman scatter lines. The Raman peak at an excitation wavelength of 348 nm (λ_{em} =380–410 nm) was measured prior to each analysis using the purified water sealed cell. All corrected data were normalised to Raman units (R.U.), allowing direct comparison of RO feed and RO permeate intensity values despite the fact that these were acquired by different instrument methods.

Pre- and post-RO fluorescent intensities were represented as excitation–emission wavelength pairs $\lambda_{ex/em}$= 240/426 nm (Peak A), 340/426 nm (Peak C), 285/350 nm (Peak T_1) and 235/350 nm (Peak T_2). The only exception was the post-RO samples from the Beenyup pilot plant where $\lambda_{ex/em}$= 300/400 nm (Peak C) and 240/400 nm (Peak A).

2.4.2. Lognormal probability plots

Lognormal probability plots were constructed to test whether the data could be fitted into a lognormal distribution. Data in the probability plot can be assumed to be lognormally distributed if the data points fit relatively well within a linear trend line. Replicate data for each sampling point were averaged and the plotting positions of these calculated according to procedures detailed previously [35]. This sampled data were then plotted as lognormal probability plots using SigmaPlot ver. 10 (Systat software, Inc) to facilitate characterisation of RO treatment variability as recommended for contaminants in water treatment facilities [36].

2.4.3. Probabilistic analysis

Once the sampled data were confirmed to be reasonably fittable to a lognormal distribution, it was fitted to cumulative lognormal probability density functions (PDFs) using @Risk ver. 5.5 software (Palisade Corporation). @Risk software was also used to generate Monte-Carlo simulations and goodness-of-fit tests. Fitted PDFs were assessed using the Anderson–Darling goodness-of-fit test, with test values less than 1 indicative of a good fit [37].

Test values for RO feed and permeate fluorescence all scored less than 1. The fitted PDFs were then used to simulate PDFs for RO percentage rejection as given in Eq. 1. Monte-Carlo simulations were undertaken using Latin Hypercube sampling with 10,000 iterations and an assumed correlation coefficient of 0.99 in sampling of RO feed and RO permeate PDFs.

$$PDF_{ROrejection(\%)} = 100 \times (PDF_{ROFeed} - PDF_{ROPermeate})/PDF_{ROFeed} \quad (1)$$

Eq.1 shows the calculation for Monte-Carlo simulation of RO rejection.

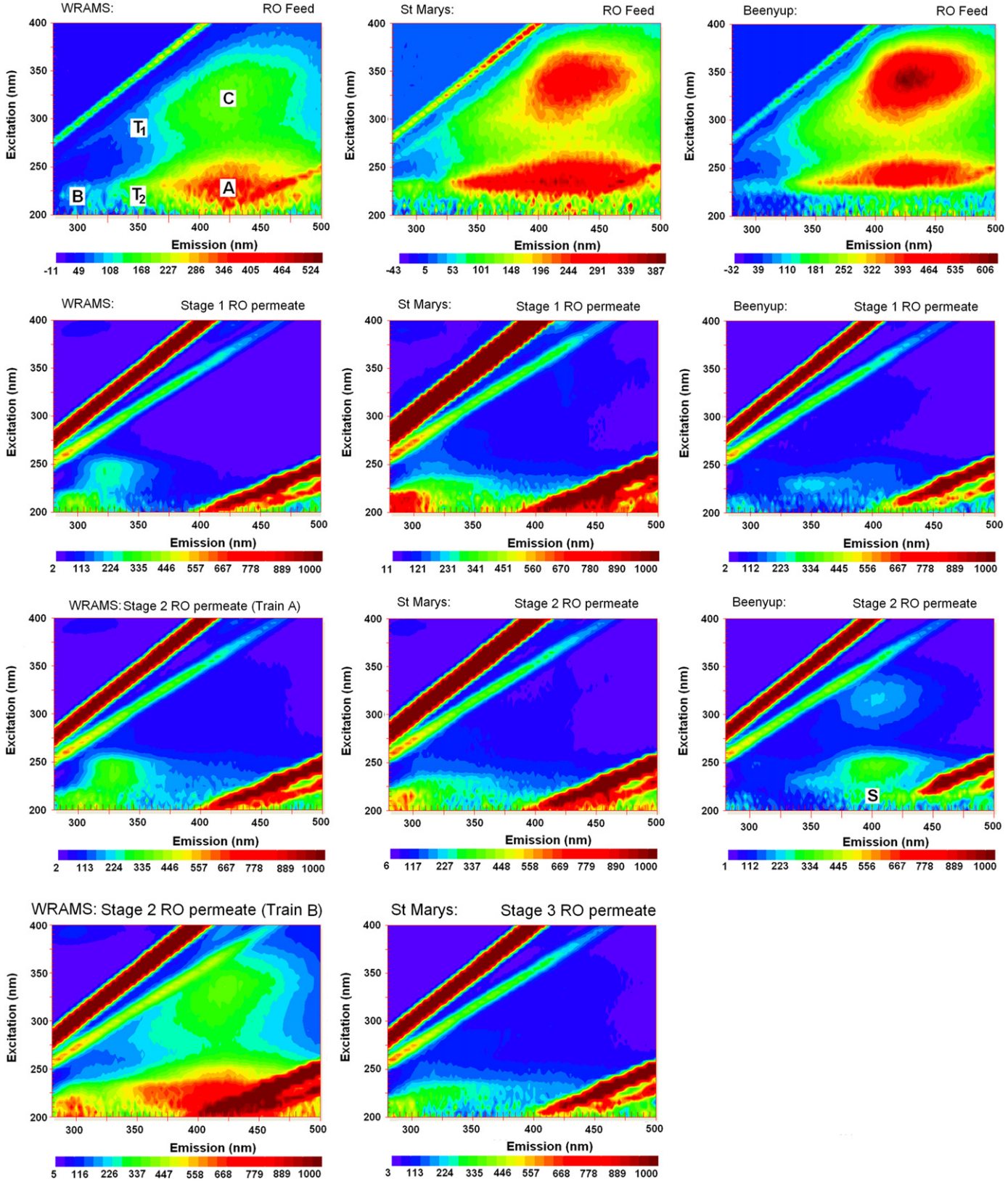

Fig. 2. Fluorescence EEMs of RO feed and RO permeates.

3. Results and discussion

3.1. Fluorescence excitation–emission matrices

The RO feed and permeate EEMs contained the five major fDOM signatures (Peaks A, C, T_1, T_2 and B) at varying intensities (Fig. 2). The predominant peaks in all RO Feed EEMs were related to humic-like fluorescence. The maxima for these are located at $\lambda_{Ex/Em}$= 340/426 nm (Peak C) and 240/426 nm (Peak A).

Post-RO EEMs, although not directly comparable with RO Feed EEMs in terms of intensity, showed significant removal of fluorescence during the RO process. Peak B was the predominant peak in all RO permeate EEMs. An exception to these were the Stage 2 permeates from the WRAMs site (Train B) which had enhanced fluorescence signatures compared to its Train A counterpart, and permeates obtained from the Beenyup pilot plant.

The dominant peaks in permeates from the Beenyup plant were related to humic-like fluorescence but the maxima for these had shifted to lower excitation and emission wavelengths (Peak C: $\lambda_{Ex/Em}$= 320/400 nm and Peak A: $\lambda_{Ex/Em}$= 240/400 nm). A small peak was also visible below Peak A at $\lambda_{Ex/Em}$= 220/400 nm. To the knowledge of the authors this peak has not been previously reported and has been labelled as Peak S. The fluorescence intensity signals for Peaks A, T_2, B and S within the RO permeates exhibited large variability between replicate samples, partially due to the noise from these regions within the EEMs, and are thus excluded from further discussion.

3.1.1. Beenyup pilot plant

Peak C, Peak T_1, EC and TOC data are presented as lognormal probability plots in Fig. 3. These charts allow visual distinction between the RO operational stages and a rudimentary assessment of exclusivity between distributions. Exclusivity between two distributions can be assessed by drawing a horizontal line across the plot. If a line can be drawn, such that it does not intersect both distributions within a defined probability range then the distributions are considered exclusive to each other.

The Stage 1 RO feed for the Beenyup plant, sourced solely from secondary treated effluent, contained the highest concentrations of fDOM among the three plants. Peak C intensities ranged from 2.5 to 7.5 R.U., while Peak T_1 ranged from 1.9 to 3.7 R.U. The RO feed also contained the highest measure of ionic species (EC=1240–2024 μScm^{-1}) in comparison to the other plants in this study, however TOC concentrations (4.8–11.0 mgL^{-1}) were at similar levels to the other plants. Stage 2 feed was the reject stream from the Stage 1 RO process and contained concentrated levels of contaminants compared to Stage 1 feed (Peak C=7.1–17.4 R.U.; Peak T_1=3.8–9.0 R.U.; EC=2897–4063 μScm^{-1}; TOC=10.2–35.5 mgL^{-1}).With the exception of TOC, all other parameters displayed exclusivity below the 90th percentile of Stage 1 feed and above the 10th percentile range of the Stage 2 RO feed (Fig. 3).

Significant removal of fDOM was observed in the permeates after RO treatment with Stage 2 permeates containing higher Peak C intensities in comparison to Stage 1. Intensities ranged from 0.02 to 0.06 R.U. for Stage 1 and 0.06 to0.09 R.U. for Stage 2. A similar trend was also observed in the EC measurements (Stage 1=14–80 μScm^{-1}; Stage 2=39–72 μScm^{-1}), with both Peak C and EC having exclusive distributions for Stage 1 ($<$90th percentile) and Stage 2 permeates ($>$10th percentile). Unlike the trend observed with the RO feeds, no distinction between permeates could be made using either Peak T_1 intensities (Stage 1=0.02–0.24 R.U.; Stage 2=0.04–0.13 R.U.) or TOC values (Stage 1=0.8–2.8 mgL^{-1}; Stage 2=0.7–2.5 mgL^{-1}).

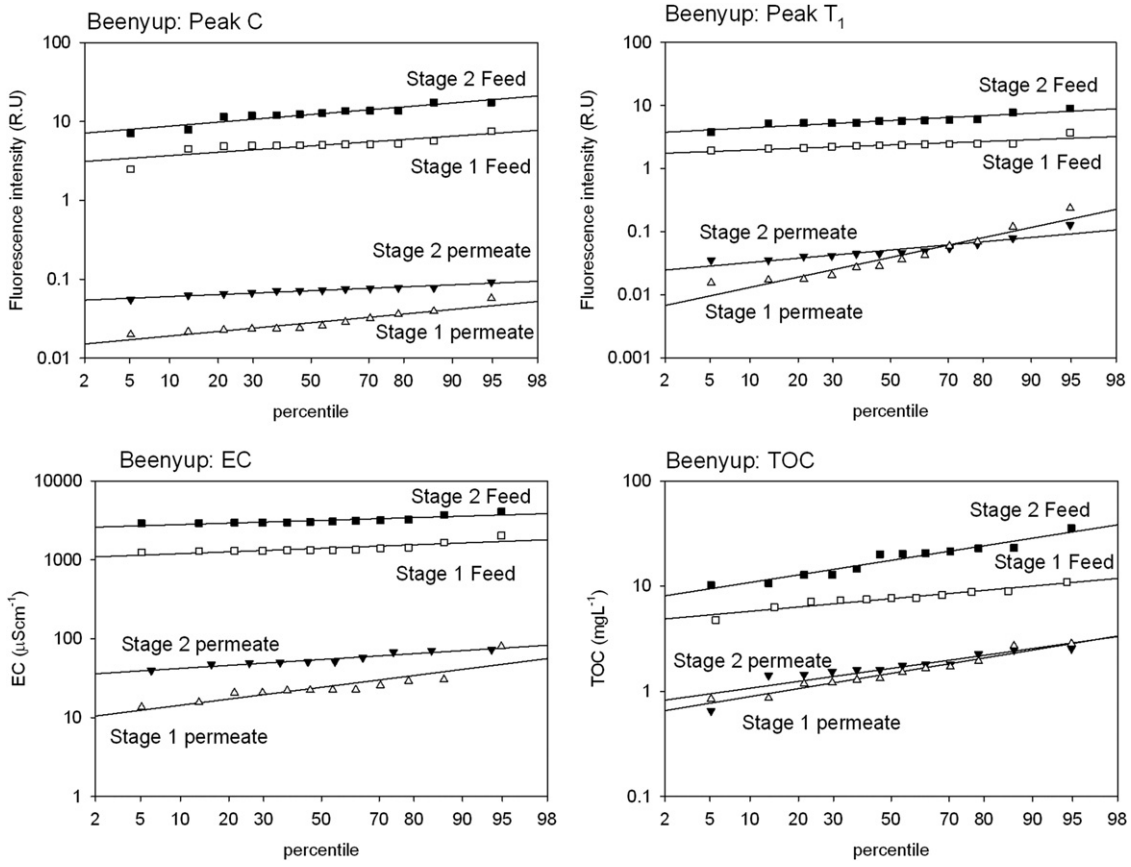

Fig. 3. Lognormal probability plots from Beenyup pilot plant.

A more distinctive feature of the RO permeates from this plant was the blue shift in the wavelength maxima for Peak C. EEM results suggest that there are two fluorophores present that fluoresce at λ_{Ex}=300 nm and at λ_{Ex}=340 nm. The fluorophores responsible for the lowered wavelength (300 nm) are retained in the permeate, while the fluorophores responsible for λ_{Ex}= 340 nm fluorescence are removed during RO. As this is trend was not observed in the other two plants this is either a unique feature of the feed water at this plant or due to reaction with chlorine.

Peak shifts have been reported to occur due to reduced aromaticity or conjugation when fDOM interacts with free chlorine [38,39]. The raw water had been exposed to chlorine (as hypochlorite) during the generation of chloramines, and it is plausible that a small portion of this chlorine has reacted with the fDOM responsible for Peak C fluorescence, with the result becoming evident after the RO process has removed most of the fDOM. The chloramination dosing involved manual input and was not accurately controlled during the pilot phase of this plant and may have been a contributing factor.

3.1.2. WRAMS treatment plant

The source water for WRAMS constituted secondary treated effluent blended with stormwater, which had a diluting effect on fluorescence and EC values. The RO feed for this plant had lower fluorescence intensities in comparison to Beenyup and a higher variability compared to St Marys, with the fDOM intensity on any day dependent on the amount of stormwater blending into the secondary effluent. Peak C fluorescence ranged from 1.4 to 3.9 R.U. while Peak T_1 ranged from 0.90 to 2.6 R.U. Lognormal probability plots are presented in Fig. 4.

Distinction between the operational stages at WRAMS could also be made using Peak C intensities in grab samples collected on the same date. The lognormal probability plots for Stage 1 permeates had Peak C intensities from 0.002 to 0.01 R.U., which partially overlapped with Peak C intensities from Train A Stage 2 permeates (0.01–0.04 R.U.). Exclusivity between stages was observed for measurements less than the 80th percentile range for Stage 1 and the greater than the 10th percentile for Stage 2 in the RO feed and permeates.

The fDOM peaks in the Train B Stage 2 permeates had enhanced fluorescence signals compared to the Train A Stage 2 permeates. It is suspected that the Train B Stage 2 modules were underperforming due to an undetermined reason. Peak C intensities (0.05–0.10 R.U.) for this were higher than the Stage 1 and Train B Stage 2 permeate intensities. This was in contrast to the Stage 1 permeates, which could not be distinguished from the two Trains. Peak T_1 signals for Stage 1 (0.01–0.04 R.U.) and Stage 2 (Train A=0.02–0.05 R.U.) permeates were indistinctive except for those sourced from Stage 2 (Train B=0.06–0.10 R.U.). Lognormal probability plots for EC and TOC showed that while EC measurements had a similar trend to Peak C fluorescence, TOC did not have the sensitivity to distinguish the operational stages and membrane underperformance (Fig. 4). The lognormal probability plots were used to assess whether the measured parameters could reliably detect the underperformance in the Stage 2 membranes within a defined signal range (Stage 1 < 90th percentile and Stage 2 > 10th percentile). TOC and Peak T_1 had overlapping distributions between the Stage 2 permeates making these unreliable parameters for this particular underperformance. Exclusivity was observed in both EC and Peak C distributions making both techniques more reliable in detecting this particular underperformance.

3.1.3. St Marys pilot plant

Lognormal probability plots for St Marys plant are presented in Fig. 5. Peak T_1 fluorescence ranged between 1.2–1.6 R.U. except

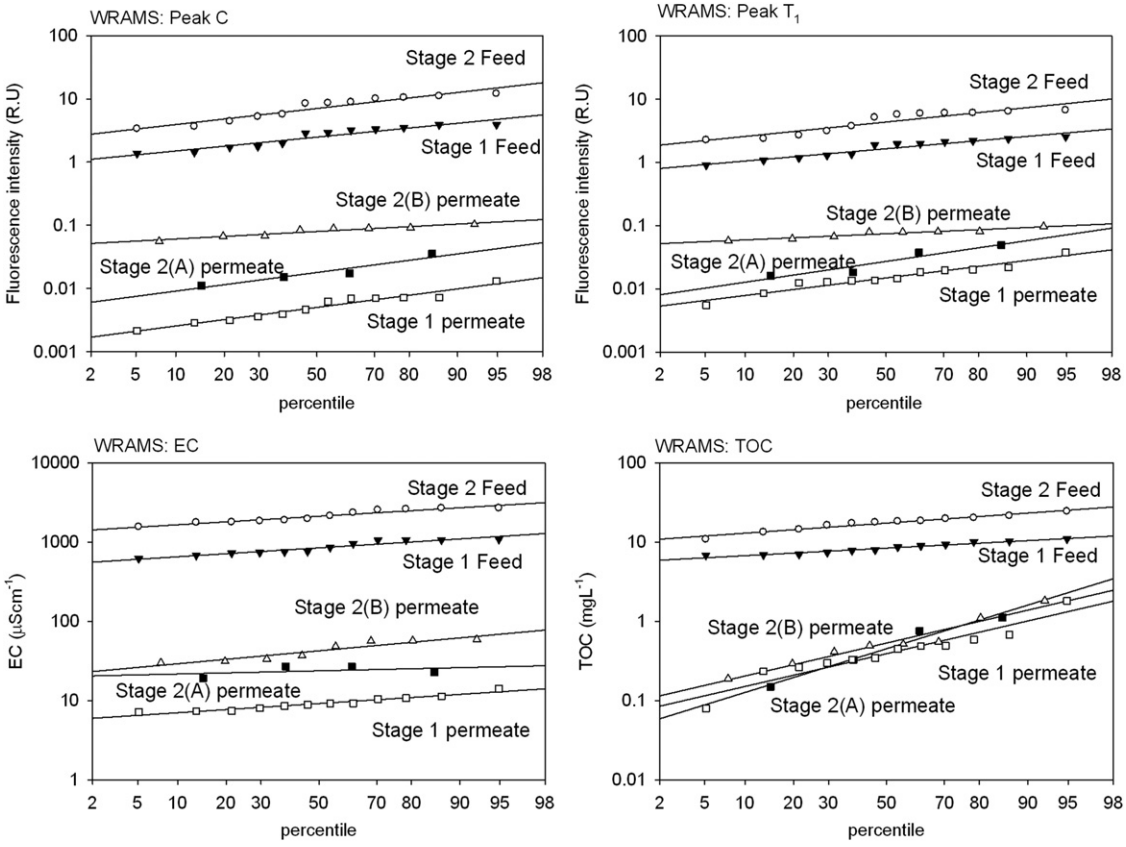

Fig. 4. Lognormal probability plots from WRAMS plant.

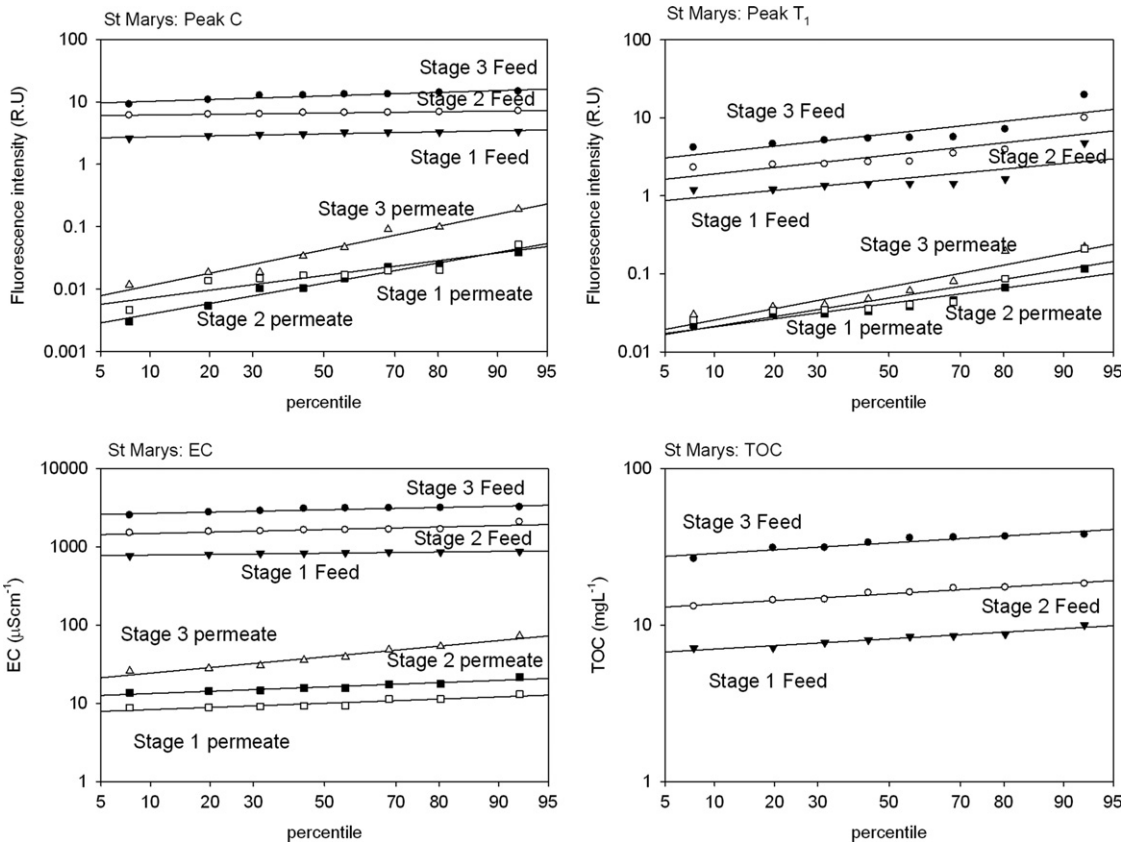

Fig. 5. Lognormal probability plots from St Marys pilot plant.

on the first sampling date, where the fluorescence averaged 4.8 R.U., the highest recorded for the three plants. This enhanced fluorescence was also observed in the RO concentrates and permeates, and may have been related to fluorescent material leached from the new membranes and plumbing, as samples collected on later dates had significantly lower T_1 fluorescence. Peak C fluorescence ranged from 2.6 to 3.4 R.U. and did not exhibit the enhanced signals observed for Peak T_1. The membranes in this plant were brand new and had been in operation for only a few days before the sampling commenced. The distributions of RO feed stages could be distinguished between the 5th^h and 95th percentile ranges using Peak C and EC.

No clear distinctions between RO stages could be made from St Marys RO permeates using fluorescence. The Stage 3 permeates generally contained higher concentrations of Peak C fluorophores (0.01–0.19 R.U.) in comparison to Stage 1 (0.005–0.05 R.U.) and Stage 2(0.003–0.04 R.U.). It is unclear if membrane age or the onset of fouling would enhance the differences between Peak C fluorescent characteristics of the RO permeate stages. Peak T_1 signals from the three RO stages were indistinctive (Stage 1=0.03–0.21 R.U., Stage 2=0.02–0.12 R.U., Stage 3=0.03–0.22 R.U.). EC distributions of the RO permeates could be distinguished ($<$90th percentile of the initial stage and $>$10th percentile of subsequent stage). No TOC data had been collected for the RO permeates.

3.1.4. Comparison between the three plants

The plant influent at the Beenyup site was sourced from secondary treated effluent and contained the highest fDOM intensities (Peak C=5.02 R.U., Peak T_1=2.32 R.U.) and EC values (1330 μScm^{-1}) as illustrated by 50th percentile values. St Marys and WRAMS sites had similar fDOM and EC values. At St Marys the plant influent was sourced from tertiary treated effluent, which had lower fDOM intensities (Peak C=3.10 R.U. and Peak T_1 =1.41 R.U.) and EC values (837 μScm^{-1}) in comparison to Beenyup. The plant influent at the WRAMS site was a blend of secondary treated effluent and stormwater, combined in daily variable proportions that had a dilution impact based on the proportion of stormwater (Peak C=2.70 R.U., Peak T_1=1.76 R.U. and EC values=826 μScm^{-1}). Peak C intensities were higher than Peak T_1 in all three feedwaters.

Pretreatment at the three sites involved either MF or UF membranes. This had no noticeable impact on DOMs and ions as described by fluorescence, DOC and EC parameters. Additionally, the plant influents at Beenyup and St Marys sites were chloraminated prior to pretreatment. However, there was no discernable impact of this on the fDOM in the RO feed. The WRAMS RO feed displayed high variability in fDOM intensities and EC compared to the other two plants due to the blending with stormwater. This was illustrated by coefficient of variation for Peak C fluorescence (Beenyup=6%, St Marys=9% and WRAMS=43%), Peak T_1 fluorescence (Beenyup=9%, St Marys=16% and WRAMS=38%) and EC (Beenyup=23%, St Marys=4% and WRAMS=33%) for the entire sampling duration.

Subsequent to RO, the Peak C intensities were lower than Peak T_1 in the permeates. RO permeates from Beenyup mimicked the trend observed with the RO feeds, and had the highest fDOM intensities (Stage 1: Peak C=0.025 R.U., Peak T_1=0.032 R.U.), EC (22.3 μScm^{-1}) and DOC (1.45 mgL^{-1}) of the three plants as shown by 50th percentile values. The lowest values were recorded for the WRAMS Stage 1 RO permeates (Peak C=0.005 R.U., Peak T_1=0.015 R.U., EC=7.0 μScm^{-1} and DOC=0.39 mgL^{-1}). Water quality parameters measured from St Marys Stage 1 permeates were intermediary between Beenyup and WRAMS (Peak C=0.017 R.U., Peak T_1=0.037 R.U. and EC=9.4 μScm^{-1}) and did not reflect the trends observed

with the RO feed. It is not known why this differs but may reflect the performances of the different RO membrane brands to the distinctive RO feeds. The impact of chloramination on the RO permeates was only observed at the Beenyup site and not at St Marys. The reason for this is unclear but it may be due differences in RO feeds or the chloramination processes.

3.2. Probabilistic analysis of fDOM removal

Probabilistic analysis was determined to be an appropriate approach for assessing RO treatment performance due to the stochastic rather than deterministic nature of fluorescent contaminants in the RO permeates, the concentrations of which had a high degree of variability and are impacted by a range of factors including pH and temperature. Summary box plots of the simulated distributions for Peak C and Peak T_1 removal by RO are presented in Fig. 6. Most of the fDOM was removed during RO, with over 98% removal (50th percentile) observed at all three plants. Peak C was better rejected by RO compared to Peak T_1, with at least 97% removal achieved at the three plants. The most consistent rejection of all parameters (based on distribution spreads) was observed at the WRAMS plant, but it cannot be ascertained whether this was a feature of the RO membranes used at this plant or due to other operational factors.

The difference in performance of the Stage 2 membranes at the WRAMS site was evident with less efficient removal of fDOM by Train B membranes compared to Train A membranes. By computing the difference between the median values (50th percentile) of the two PDFs it was observed that Peak T_1 rejection was 1.0% lower in Train B compared to Train A while Peak C was 0.8% lower. Peak C % removal PDFs of the two Trains were exclusive to each other for values less than 95th percentile values (Peak C=99.2%), of Train B and values greater than 5th percentile (Peak C=99.5%) of Train A. Peak T_1% removal PDFs had a small degree of overlap between the 95th percentile values of Train B (99.8%) and the 5th percentile values of Train A (98.8%). EC rejection distributions confirmed lowered performance in the Stage 2 Train B membranes relative to Train A, however no differences could be detected based on TOC rejection.

In all three plants Peak T_1 removal appeared to improve after each subsequent operational stage. The PDFs of each stage were indistinguishable due to overlapping ranges but median values (50th percentile) increased after each operational stage. The most distinctive example of this trend was at the St Marys plant (Stage 1=97.2%, Stage 2=98.2% and Stage 3=99.0%). Beenyup (Stage 1=98.6% and Stage 2=99.2%) and WRAMS (Stage 1=99.1% and Stage 2 Train A=99.4%) plants also exhibited similar trends. Peak C removal provided no distinction between operational stages thus showing stable rejection. It is not understood why improved rejection of Peak T_1 was achieved after each subsequent RO stage. At the St Marys plant the Stage 1 Peak T_1 removal exhibited a high degree of variability. The distributions for these were skewed by the high Peak T_1 concentrations found in feed and permeate in the first two sets of samples. It appears that a longer stabilisation period for Peak T_1 is required compared to Peak C for optimum rejection to be achieved by new membranes.

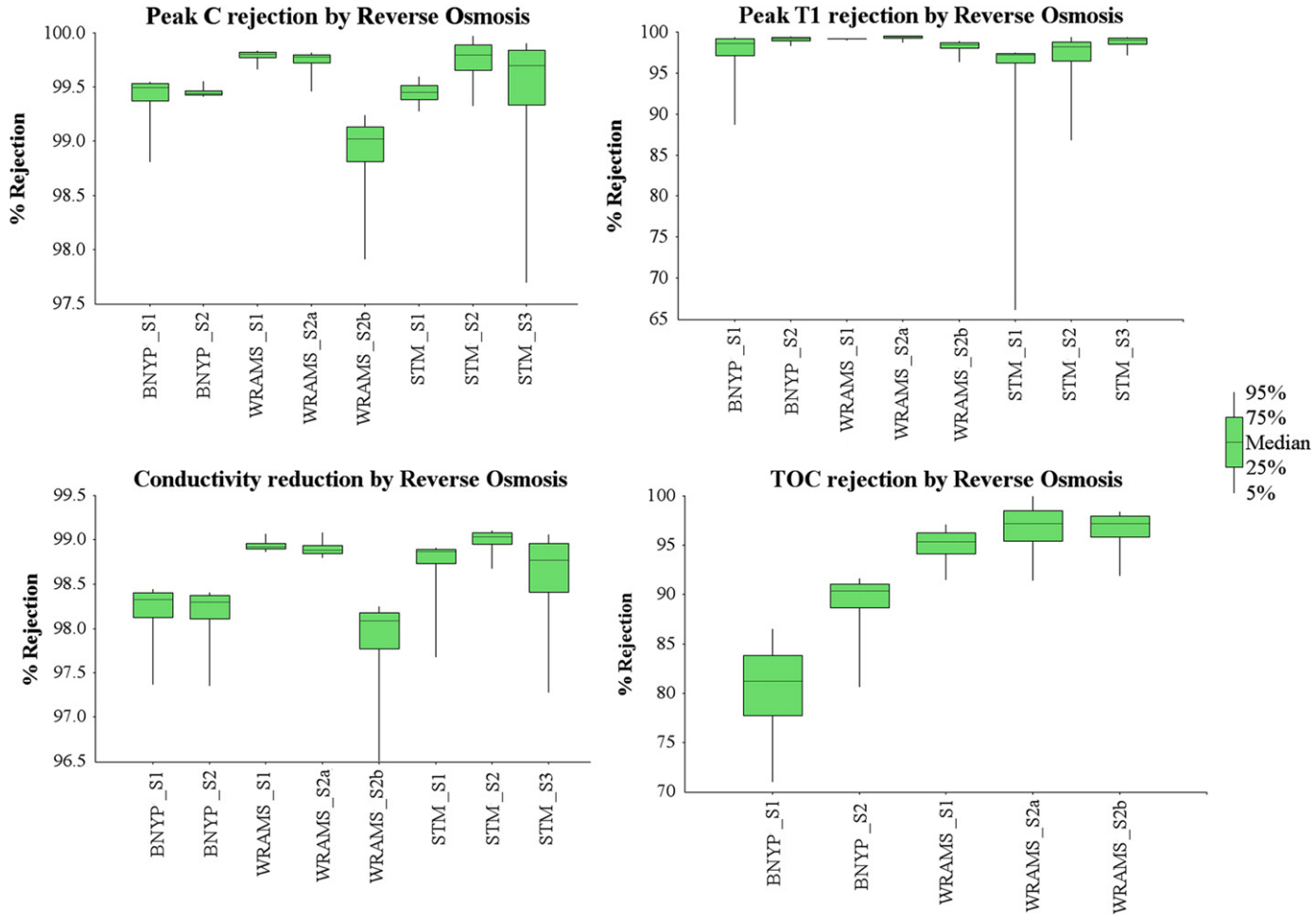

Fig. 6. Summary box plots of simulated distributions for fDOM removal by reverse osmosis.

3.3. Implications for integrity monitoring

Peak C at $\lambda_{Ex/Em}$= 340/426 nm appears to be best suited for RO membrane performance and integrity monitoring. This fluorescent region is responsive to the differences in feed quality as observed by the differences in Stage 1 and Stage 2 permeates, showing sensitivity to subtle changes in permeate characteristics. More importantly, it demonstrates high sensitivity to membrane underperformance as observed in the enhanced intensities of the Train B Stage 2 permeates from the WRAMS site. Peak C was the only fluorescence region that no overlapping intensities between Train A and Train B permeates (5th–95th percentile range). RO rejection data corroborated this with a clear and distinct reduction in RO rejection observed for the same permeates.

It is possible to collect near-real time EEMs; the method employed in this study requires 5 min to generate an EEM. However, the cost of spectrophotometers and the skill and maintenance requirements (with or without multivariate data analyses) may be difficult for many utilities to implement. Monitoring these smaller wavelength regions or specific excitation–emission coordinate pairs provide as much relevant information as full EEMs coupled with multivariate datamining tools for process performance monitoring [34]. In the current study five distinct fDOM peaks were detected, three of which were in regions of high noise and did not provide consistent results (Peak A, Peak B and Peak T_2). More consistent results were obtained from Peak C and Peak T_1. Of these, Peak C was more sensitive to subtle changes in RO permeate quality. Thus no significant advantage can be obtained from monitoring full EEMs in comparison to smaller wavelength regions.

Several fluorescence sensors which measure only a small fluorescence band are available on the market. Many of these use light emitting diode (LED) technology, which has significantly improved sensitivity and reduced costs to below AU$10,000, making these economically competitive to technology such as TOC analysers, which can cost over AU$40,000. These can be more easily implemented into RO plants and provide a simple signal output that can trigger an alarm when designated critical control points are exceeded. One such low cost fluorometer, the Cyclops 7 CDOM sensor (Turner Designs) has been identified for future online monitoring trials. This sensor measures fluorescence at $\lambda_{Ex/Em}$= 350/430 nm (Peak C region) and was obtained for AU$2500.

Fluorescence peak maxima shifts observed from addition of chlorine/chloramines can be potentially problematic to account for using portable fluorescence instruments capable of measuring only within a limited wavelength region. These regions are typically selected by bandpass filters which cover a small range of excitation and emission and not a specific wavelength pair. Also the output is usually the maximum emission signal detected within that range. The user can have the choice when purchasing equipment to either obtain instruments with interchangeable, broad bandpass filters; or to select an instrument with a fixed bandpass that covers the range required. This range should ideally include the peak maxima wavelength pairs from before and after the peak shift. It should also be noted that an exact match to the wavelength coordinate pair used in this study is not essential. The fDOM peaks are broad and cover a relatively large area of optical space within the EEM. The decrease in fluorescence intensity from the peak maxima is gradual and a strong signal can still be obtained from wavelength coordinate pairs that are located several nanometres from the peak maxima. Finally, in an integrity loss scenario it is expected that DOM responsible for fluorescent maxima signatures (prior to the peak shift) would not be removed as efficiently and enter the permeate stream in higher concentrations. Thus it is likely to mask out any effects of the peak shift.

4. Conclusions

In this study, the fluorescence signatures of RO feed and permeate samples sourced from three municipal recycled water treatment facilities were analysed and characterised. Multiple peaks were identified including the novel peak S at $\lambda_{Ex/Em}$= 220/400 nm. Peak C and Peak T_1 were identified as suitable for investigative purposes due to relatively low noise and variability in replicate samples and the rejection of these fluorescent organic molecules was assessed by Monte-Carlo analysis.

It was found that the Peak C was better rejected by RO than Peak T_1 although typical rejection for both peaks was over 98%. Peak T_1 rejection appeared to improve after each subsequent RO stage although the reason for this could not be determined. Peak T_1 also requires a longer stabilisation period compared to Peak C when new membranes are commissioned as observed from the rejection trends for the St Marys plant. Peak C was determined to better suited for RO performance monitoring than Peak T_1 based on the exclusivity of underperforming membrane fDOM rejection PDFs and the permeate fluorescence intensity PDFs to those of unimpaired membrane. RO feed samples from different operational stages could be distinguished based on Peak C and Peak T_1 intensities. In contrast, only Peak C could be used to distinguish permeates from different operational stages which were only valid for two of the plants in this study. This is attributed to the improving rejection of Peak T_1 at each subsequent RO stage.

Results in this study show fluorescence has the capability of detecting subtle changes in RO permeates. This demonstrates that monitoring a small fluorescence region or excitation–emission coordinate pair would be more practical than measuring full EEMs. This will also make it easier and more cost effective to implement in water utilities using RO and flags the potential for fluorescence-based online monitoring of RO performance.

Acknowledgements

This sampling programme was funded by the Australian Research Council linkage projects funding scheme (LP0776347)—Sydney Water Corporation, Sydney Olympic Park Authority, Allconnex Water, Melbourne Water, City West Water, South East Water and Water Corporation. The authors would like to thank Mark Handyside (Water Corp), Simon Higginson (Water Corp), Palenque Blair (Water Corp), Michael James (United KG), Ralph Wardell (United KG), Matthew Schubach (United KG), James McDonald (UNSW) and Karen McGeough (UNSW) for their assistance in sample and data collection. Gratitude is also expressed to Dr. Kathleen Murphy for designing the initial Matlab correction files.

References

[1] T. Wintgens, T. Melin, A. Schäfer, S. Khan, M. Muston, D. Bixio, C. Thoeye, The role of membrane processes in municipal wastewater reclamation and reuse, Desalination 178 (2005) 1–11.
[2] National, Water, Quality, Management, Strategy, Australian Guidelines for Water Recycling: Managing Health and Environmental Risks (Phase 1), Natural Resource Management Ministerial Council, Environmental Protection and Heritage Council, Australian Health Minister's Conference, Canberra, 2006.
[3] C. Bellona, J.E. Drewes, P. Xu, G. Amy, Factors affecting the rejection of organic solutes during NF/RO treatment—a literature review, Water Res. 38 (2004) 2795–2809.
[4] L.D. Nghiem, S. Hawkes, Effects of membrane fouling on the nanofiltration of trace organic contaminants, Desalination 236 (2009) 273–281.
[5] L.D. Nghiem, P.J. Coleman, C. Espendiller, Mechanisms underlying the effects of membrane fouling on the nanofiltration of trace organic contaminants, Desalination 250 (2010) 682–687.

[6] S. Adham, P. Gagliardo, D. Smith, D. Ross, K. Gramith, R. Trussell, Monitoring the integrity of reverse osmosis membranes, Desalination 119 (1998) 143–150.
[7] M. Kumar, S. Adham, J. DeCarolis, Reverse osmosis integrity monitoring, Desalination 214 (2007) 138–149.
[8] R.G. Godec, P.P. Kosenka, B.D. Smith, R.S. Hutte, J.V. Webb, R.L. Sauer, Total organic carbon analyzer, in: Proceedings of the 21st International Conference on Environmental Systems, SAE, San Francisco, CA, USA, 1991, pp. 103–114.
[9] Ionics launches TOC analyzers, Membrane Technology, (2004) 3.
[10] R.K. Henderson, R.M. Stuetz, S.J. Khan, Demonstrating ultra-filtration and reverse osmosis performance using size exclusion chromatography, Water Sci. Tech. 62 (2010) 2747–2753.
[11] E.M. Carstea, A. Baker, G. Pavelescu, I. Boomen, Continuous flourescence assessment of organic matter variability on the Bournbrook River, Birmingham, UK, Hydrol. Process. 23 (2009) 1937–1946.
[12] T. Kuzniz, D. Halot, A.G. Mignani, L. Ciaccheri, K. Kalli, M. Tur, A. Othonos, C. Christofides, D.A. Jackson, Instrumentation for the monitoring of toxic pollutants in water resources by means of neural network analysis of absorption and fluorescence spectra, Sens. Actuators B Chem. 121 (2007) 231–237.
[13] P. Lambert, M. Goldthorp, B. Fieldhouse, Z. Wang, M. Fingas, L. Pearson, E. Collazzi, Field fluorometers as dispersed oil-in-water monitors, J. Hazard. Mater. 102 (2003) 57–79.
[14] R.K. Henderson, A. Baker, K.R. Murphy, A. Hambly, R.M. Stuetz, S.J. Khan, Fluorescence as a potential monitoring tool for recycled water systems: a review, Water Res. 43 (2009) 863–881.
[15] Y. An, Z. Wang, Z. Wu, D. Yang, Q. Zhou, Characterization of membrane foulants in an anaerobic non-woven fabric membrane bioreactor for municipal wastewater treatment, Chem. Eng. J. 155 (2009) 709–715.
[16] S. Ciputra, A. Antony, R. Phillips, D. Richardson, G. Leslie, Comparison of treatment options for removal of recalcitrant dissolved organic matter from paper mill effluent, Chemosphere 81 (2010) 86–91.
[17] H. Zhang, J. Qu, H. Liu, X. Zhao, Characterization of isolated fractions of dissolved organic matter from sewage treatment plant and the related disinfection by-products formation potential, J. Hazard. Mater. 164 (2009) 1433–1438.
[18] D.A. Skoog, D.M. West, F.J. Holler, S.R. Crouch, Fundamentals of Analytical Chemistry, Brooks/Cole-Thomson Learning, Belmont, CA, 2004.
[19] J.J. Mobed, S.L. Hemmingsen, J.L. Autry, L.B. McGown, Fluorescence characterization of IHSS humic substances: Total luminescence spectra with absorbance correction, Environ. Sci. Technol. 30 (1996) 3061–3065.
[20] A. Baker, Fluorescence excitation–emission matrix characterization of some sewage-impacted rivers, Environ. Sci. Technol. 35 (2001) 948–953.
[21] P.G. Coble, Characterization of marine and terrestrial DOM in seawater using excitation–emission matrix spectroscopy, Mar. Chem. 51 (1996) 325–346.
[22] A. Baker, Fluorescence excitation-–emission matrix characterization of river waters impacted by a tissue mill effluent, Environ. Sci. Technol. 36 (2002) 1377–1382.
[23] N. Hudson, A. Baker, D. Ward, D.M. Reynolds, C. Brunsdon, C. Carliell-Marquet, S. Browning, Can fluorescence spectrometry be used as a surrogate for the biochemical oxygen demand (BOD) test in water quality assessment? An example from South West England, Sci. Total Envir. 391 (2008) 149–158.
[24] T. Jiang, M.D. Kennedy, V.D. Schepper, S.N. Nam, I. Nopens, P.A. Vanrolleghem, G. Amy, Characterization of soluble microbial products and their fouling impacts in membrane bioreactors, Environ. Sci. Technol. 44 (2010) 6642–6648.
[25] K. Kimura, T. Naruse, Y. Watanabe, Changes in characteristics of soluble microbial products in membrane bioreactors associated with different solid retention times: Relation to membrane fouling, Water Res. 43 (2009) 1033–1039.
[26] S. Tang, Z. Wang, Z. Wu, Q. Zhou, Role of dissolved organic matters (DOM) in membrane fouling of membrane bioreactors for municipal wastewater treatment, J. Hazard. Mater. 178 (2010) 377–384.
[27] Z. Wang, Z. Wu, S. Tang, Characterization of dissolved organic matter in a submerged membrane bioreactor by using three-dimensional excitation and emission matrix fluorescence spectroscopy, Water Res. 43 (2009) 1533–1540.
[28] C.F. Galinha, G. Carvalho, C.A.M. Portugal, G. Guglielmi, R. Oliveira, J.G. Crespo, M.A.M. Reis, Real-time monitoring of membrane bioreactors with 2D-fluorescence data and statistically based models, Water Sci. Tech. 63 (2011) 1381–1388.
[29] G. Wolf, J.S. Almeida, J.G. Crespo, M.A.M. Reis, An improved method for two-dimensional fluorescence monitoring of complex bioreactors, J. Biotechnol. 128 (2007) 801–812.
[30] N. Lee, G. Amy, J.P. Croué, Low-pressure membrane (MF/UF) fouling associated with allochthonous versus autochthonous natural organic matter, Water Res. 40 (2006) 2357–2368.
[31] R.H. Peiris, H. Budman, C. Moresoli, R.L. Legge, Understanding fouling behaviour of ultrafiltration membrane processes and natural water using principal component analysis of fluorescence excitation–emission matrices, J. Membr. Sci. 357 (2010) 62–72.
[32] B.R.H. Peiris, C. Halle, J. Haberkamp, R.L. Legge, S. Peldszus, C. Moresoli, H. Budman, G. Amy, M. Jekel, P.M. Huck, Assessing nanofiltration fouling in drinking water treatment using fluorescence fingerprinting and LC-OCD analyses, Water Sci.Technol.: Water Supply 8 (2008) 459–465.
[33] S. Singh, R.K. Henderson, A. Baker, S.J. Khan, R.M. Stuetz, Distinguishing stage 1 and 2 reverse osmosis permeates using fluorescence spectroscopy, Water Sci. Technol. 60 (2009) 2017–2023.
[34] K.R. Murphy, A. Hambly, S. Singh, R.K. Henderson, A. Baker, R. Stuetz, S.J. Khan, Organic matter fluorescence in municipal water recycling schemes: toward a unified PARAFAC model, Environ. Sci. 45 (2011) 2909–2916.
[35] S.J. Khan, Quantitative chemical exposure assessment for water recycling schemes, Waterlines Report Series No. 27, 2010, pp.87–88.
[36] D. Eisenberg, J. Soller, R. Sakaji, A. Olivieri, A methodology to evaluate water and wastewater treatment plant reliability, Water Sci. Technol. 43 (2001) 91–99.
[37] T.W. Anderson, D.A. Darling, Asymptotic theory of certain goodness of fit criteria based on stochastic processes, Ann. Math. Stat. 23 (1952) 193–212.
[38] P. Roccaro, F.G.A. Vagliasindi, G.V. Korshin, Changes in NOM fluorescence caused by chlorination and their associations with disinfection by-products formation, Environ. Sci. Technol. 43 (2009) 724–729.
[39] S. Xue, K. Wang, Q.L. Zhao, L.L. Wei, Chlorine reactivity and transformation of effluent dissolved organic fractions during chlorination, Desalination 249 (2009) 63–71.